

# V404 Cygni with *Fermi*-LAT

Max Harvey <sup>\*</sup>, Cameron B. Rulten  and Paula M. Chadwick 

*Centre for Advanced Instrumentation, Department of Physics, University of Durham, South Road, Durham DH1 3LE, UK*

Accepted 2021 July 14. Received 2021 July 14; in original form 2020 November 17

## ABSTRACT

We revisit the well-studied outburst of the low-mass X-ray binary (LMXB) system V404 Cygni, and claims of  $\gamma$ -ray excesses observed with the *Fermi*-LAT instrument. Upon analysing an 11.5 yr data set with the 8-yr LAT point source catalogue and 8-yr background models, we find no evidence to suggest that there is high energy  $\gamma$ -ray emission during the outburst period (or at any other time) from V404 Cygni. This is due to the proximity of V404 Cygni to the  $\gamma$ -ray emitting blazar B2023+336, a luminous source approximately  $0.3^\circ$  away, which causes source confusion at the position of V404 Cygni, the luminous  $\gamma$ -ray background, and the use of older background models and catalogues in previous studies.

**Key words:** black hole physics – gamma-rays: stars – X-rays: binaries.

## 1 INTRODUCTION

### 1.1 X-ray binaries and $\gamma$ -ray emission

V404 Cygni (also known as GS 2023+338) is an X-ray binary system that lies on the Galactic plane (Kitamoto et al. 1989). It consists of a K-type star with a mass slightly below  $1 M_\odot$  (Wagner et al. 1992) and a black hole companion of mass  $9 M_\odot$  (Khargharia, Froning & Robinson 2010); this stellar mass means that V404 Cygni is considered a low-mass X-ray binary (LMXB). This system is visible across the EM spectrum, with X-ray emission originating from accretion of the donor star on to its black hole companion; in common with other LMXBs, the accretion occurs through overflow of the star's Roche lobe on to the black hole.

High energy  $\gamma$ -ray emission has been observed from a variety of binary systems, with the emission thought to originate in one of three mechanisms. In the first, the spin-down of young pulsars causes  $\gamma$ -ray emission through relativistic shocks (Dubus 2006), these systems are typically referred to as  $\gamma$ -ray binaries. The second type of system is a colliding wind binary, where interactions between the stellar winds of two massive stars produce  $\gamma$ -rays up to TeV energies. The only colliding wind binary detected with *Fermi*-LAT is  $\eta$ -Carinae (Leser et al. 2017). Finally, a class of binaries known as the microquasars is predicted to produce  $\gamma$ -rays through the acceleration of particles in jets (Bosch-Ramon, Romero & Paredes 2006, Orellana et al. 2007, Araudo, Bosch-Ramon & Romero 2009). Jets are seen from microquasars in a variety of states as described by the hardness-intensity cycle (Fender, Belloni & Gallo 2004), including compact jets in the low-hard X-ray state (Tomsick et al. 2008). It is from these jets that the particle acceleration required for  $\gamma$ -ray emission takes place, with evidence to suggest that  $\gamma$ -rays are produced when a jet forms at the transition between the hard and soft state, and also from the hard state compact jet (Zdziarski et al. 2017).

There are a number  $\gamma$ -ray emitting microquasar objects known. The first and arguably best studied is SS 433, which is a unique

case as it is the only X-ray binary known to accrete in a constant supercritical way (Fabrika 2004). Other well-known  $\gamma$ -ray emitting microquasars more comparable to V404 Cygni include Cygnus X-3 (Tavani et al. 2009) [where orbital  $\gamma$ -ray modulation is seen (Abdo et al. 2009)] and Cygnus X-1, where  $\gamma$ -ray emission is seen during the hard spectral state (Bodaghee et al. 2013, Zanin et al. 2016, Zdziarski et al. 2017). As V404 Cygni is not in a supercritical accretion regime, it is thought to produce  $\gamma$ -ray emission through entering an outburst like Cygnus X-1 and Cygnus X-3.

### 1.2 Outbursts of V404 Cygni

There have been at least three historic outbursts of V404 Cygni during the 20th Century: one in 1938 (when the system was designated Nova Cygni 1938), one in 1958 (undetected at the time), a possible outburst in 1979, and the well-studied outburst of 1989 (Duerbeck 1988; Makino 1989; Richter 1989; Wagner et al. 1989; Han & Hjellming 1992). Together with the 2015 outburst, this means that V404 Cygni has an outburst approximately every few decades. Prior to the 1989 outburst, these events were recorded only in the optical waveband; the 1989 outburst was also captured in the X-ray waveband by the *Ginga* X-ray Astronomy Satellite and the system was designated GS 2023+338 (Kitamoto et al. 1989). The simultaneous X-ray and optical activity of the 1989 outburst led to the rapid association of GS 2023+338 with V404 Cygni (Wagner et al. 1989).

In 2015 June, *Swift*-BAT reported that V404 Cygni had begun an outburst with enhanced fluxes reported across the spectrum, with *Fermi*-GBM triggering approximately 30 min later. At this time, an enhancement in accretion rate caused a subsequent enhancement in jet brightness, sending V404 Cygni into an outburst. Before it returned to its pre-outburst flux level in 2015 August, INTEGRAL, *Swift*, AGILE, MAGIC, and VERITAS all took observations at high energies, with *Fermi*-LAT's all sky coverage also capturing the position of V404 Cygni during its outburst. There was also a brief 'sequel' flare in 2015 December, lasting for approximately 2 weeks. However, for the purposes of this paper we consider the outburst as exclusively within the 2015 June–2015 August period.

\* E-mail: max.harvey@durham.ac.uk

The *Swift* team reported a variable X-ray flux, at times in excess of 40 times the Crab Nebula flux (Barthelmy et al. 2015, Motta et al. 2017), in addition to enhanced and variable UV and optical fluxes (Oates et al. 2019). Enhanced fluxes from the V-band optical up to the soft  $\gamma$ -rays (40–100 keV) were observed with INTEGRAL (Rodríguez et al. 2015; Roques et al. 2015). The AGILE (50–400 MeV  $\gamma$ -ray) team reported a  $4.3\sigma$  enhancement of  $\gamma$ -ray flux, contemporaneous with a large flare in the radio and X-ray wavebands between MJD 57197.25–57199.25, though no significant  $\gamma$ -ray emission above 400 MeV was reported (Piano et al. 2017), with a similar excess also being observed with *Fermi*-LAT (Loh et al. 2016). In the very high energy (GeV to TeV) range, the VERITAS (Archer et al. 2016) and MAGIC collaborations (Ahnen et al. 2017) both reported upper limits from the position of V404 Cygni.

## 2 V404 CYGNI AS SEEN WITH *FERMI*-LAT

The *Fermi*-LAT has an effective energy range of 100 MeV to 300 GeV, which essentially bridges the gap in energy between AGILE (operating in the MeV range) and Cherenkov telescope systems like VERITAS and MAGIC (operating in the GeV–TeV range). Although a  $4.3\sigma$  enhanced  $\gamma$ -ray flux was below 400 MeV was seen with AGILE, there was no significant detection over the 10 hr exposure of MAGIC (VERITAS had a shorter exposure of 2.5 hr). It is questionable whether one would expect to see an enhanced flux with *Fermi*-LAT.

At the position of V404 Cygni, there is no catalogued source in the most recent *Fermi*-LAT point source catalogue, the 4FGL (Abdollahi et al. 2020). This is to be expected, as the 4FGL uses an 8 yr observation time to detect sources, whereas we might expect high energy  $\gamma$ -rays to be produced only when V404 Cygni is in an outburst. Even if V404 Cygni was luminous in  $\gamma$ -rays throughout its outburst, the long observation time would render this emission insignificant.

However, the 4FGL does catalogue a luminous  $\gamma$ -ray emitting flat spectrum radio quasar (FSRQ), B2023+336, approximately  $0.3^\circ$  away from the position of V404 Cygni, detected through the Galactic plane (Kara et al. 2012). This is problematic, as the resolution of the LAT varies from between an optimal  $0.15^\circ$  at  $>10$  GeV down to a substantially poorer resolution of  $3.5^\circ$  at 100 MeV (see fig. 17 in Atwood et al. 2009). As a result, source confusion between B2023+336 and V404 Cygni becomes the primary issue in reliably detecting  $\gamma$ -ray emission from the LMXB with *Fermi*-LAT at any but the highest energies. In addition, V404 Cygni is located on the Galactic plane, a significant steady source of background photons, which are non-trivial to model, although the most recent Galactic diffuse model improves on previous releases (Abdollahi et al. 2020). This presents additional challenges to resolving any  $\gamma$ -ray emission from V404 Cygni.

### 2.1 The results of Loh et al. and Piano et al.

Loh et al. (2016, referred to as Loh 16 throughout this text) explore the *Fermi*-LAT data in the period around the outburst of V404 Cygni, performing a comprehensive variability analysis at the position of V404 Cygni. They use photons across most of the *Fermi*-LAT energy spectrum (100 MeV to 100 GeV), but discard the quartile of photons with the poorest point spread function (PSF) label. While this allows for the better localization of remaining  $\gamma$ -ray emission in a model, significant cuts to the number of photons make it more difficult to detect sources, particularly faint and transient ones such V404 Cygni.

Loh 16 perform a variability analysis on the position of V404 Cygni by first carrying out a binned analysis of the region

and then executing an unbinned light-curve time-series analysis. The bins used are 12 hr (shifted by 6 hr), and 6 hr (shifted by 1 hr) in duration. Based on these results, an excess in the  $\gamma$ -ray flux is found near the position of V404 Cygni with a peak test statistic (TS) of 15.3 in one particular 6 hr bin at approximately MJD 57199. The TS of the 12 hr bin containing this 6 hr bin is approximately 11. The authors describe this transient excess of having a chance probability of occurring as 2 per cent (giving a  $z$ -score of approximately  $2\sigma$ ) based on 320 trials. They state that this gives a  $4 \times 10^{-4}$  chance probability of occurring at the same time as a peak in the *Swift*-BAT flux light curve. For the purposes of this paper, we will describe this event as the June 2015 excess.

The analysis of Loh 16 used the most up-to-date models and catalogues for the *Fermi*-LAT data at the time: the `gll_iem_v06` Galactic background model, the `iso_p8r2_source_v6_v06` isotropic background model, and the 3FGL catalogue and extended source templates. Improved background models, the 4FGL catalogue, and improved instrument response functions (IRFs) for the LAT are now available. These allow for an improved analysis of the *Fermi*-LAT data at the time and position of the V404 Cygni outburst.

Loh 16 is not the only paper discussing the June 2015 excess as seen with *Fermi*-LAT. Piano et al. (2017, hereafter Piano 17), while discussing this same event as seen with the AGILE  $\gamma$ -ray Imaging Detector (GRID), provide an independent *Fermi*-LAT analysis that complements both the results from the AGILE telescope and those of Loh 16. In the analysis of the AGILE data, Piano 17 consider photons in two energy bands: 50 MeV–400 MeV and 400 MeV–30 GeV. Piano 17 record a  $\gamma$ -ray excess of  $TS = 18.1$ , ( $4.3\sigma$  for 1 degree of statistical freedom) in this first energy band, at a time coincident with the excess recorded by Loh 16. There is no detection at energies  $>400$  MeV.

In their *Fermi*-LAT analysis, Piano 17 use a different set of photon cuts to Loh 16. They analyse photons across all 4 PSF quartiles, using the `P8R2_TRANSIENT_v16` photon class with the same background models as Loh 16 (the `gll_iem_v06` Galactic model and `iso_p8r2_source_v6_v06` isotropic model). Piano 17 report a TS of 13.4 in the 24 hr period from MJD 57198.75–57199.75, temporally coincident with the result of Loh 16.

Each *Fermi*-LAT photon class has a corresponding isotropic model and IRF, and it is good practice when carrying out LAT data analysis to use these together. Piano 17 use the `P8R2_TRANSIENT_v16` photon class with the `iso_p8r2_source_v6_v06` isotropic model, and an unspecified IRF. The use of a mismatched isotropic background and photon class will result in systematic errors in source analysis, and in the misidentification of cosmic rays, reducing the accuracy of Piano 17's results, though without knowing the IRF it is difficult to assess by how much. Consequently, we primarily deal with the LAT results from Loh 16 in this paper, as they do not have this additional uncertainty, and find more significant  $\gamma$ -ray emission at the LAT data from the position of V404 Cygni.

### 2.2 The results of Xing and Wang

In a more recent paper, Xing & Wang (2020, henceforth referred to as Xing 20), carried out an analysis of the *Fermi*-LAT data, independent to that of Loh 16. Xing 20 employ the most recent 4FGL catalogue and corresponding background models to perform a variability analysis over the mission time of the *Fermi* satellite.<sup>1</sup>

<sup>1</sup>It should be noted that at the time of publication, Xing 20 is available only at [arxiv.org](https://arxiv.org), and has not been published in a peer reviewed journal.

**Table 1.** The parameters used in the likelihood analysis of the region of interest (ROI) around V404 Cygni.

Observation Period (Dates)	04/08/2008–10/01/2020
Observation Period (MET)	239557417–600307205
Observation Period (MJD)	54682–58423
Energy Range (GeV)	0.1–300
evtype	3 (FRONT + BACK)
evclass	128 (P8R3_SOURCE)
Data ROI width	25°
Model ROI Width	30°
Zenith Angle	<90°
Instrument Response	P8R3_SOURCE_V2
Isotropic Background Model	iso_P8R3_SOURCE_V2_v1
Galactic Background Model	gll_iem_v07
Point Source Catalogue	4FGL

In order to test the results of Loh 16, the authors repeat their variability analysis using a similar overlapping time binning scheme at the same time, using a binned analysis. Xing 20 do not state which event class and event type were used in their LAT data analysis. They find no significant  $\gamma$ -ray flux at the peak of the *Swift*-BAT X-ray flux (on MJD 57199), which is the result of Loh 16. Xing 20 suggests that the June 2015  $\gamma$ -ray excess of Loh 16 was a result of employing older (and poorer) catalogue, background models and IRF, rather than a genuine  $\gamma$ -ray flare. The lack of detail concerning the analysis parameters and the lack of TS maps below 300 MeV (where the flux of the  $\gamma$ -ray emission reported by Loh 16 is highest) make it very difficult to reproduce the results of Xing 20.

Xing 20 do claim a separate  $\gamma$ -ray excess (TS  $\approx$  15) during August 2015, which is towards the end of the V404 Cygni outburst (henceforth referred to as the August 2015 excess). This analysis does not account for any photons with an energy less than 300 MeV, in contrast to the Xing 20 analysis of the June 2015 excess. More significantly, they claim detection of  $\gamma$ -ray emission from V404 Cygni at the  $7\sigma$  level in August 2016 (the August 2016 excess). This is approximately a year after the June 2015 outburst finishes, and Xing 20 report that there is no corresponding increase in X-ray flux in the *Swift*-BAT light curve at this time.

In this paper, we provide an independent analysis of the reported V404 Cygni  $\gamma$ -ray excesses, and of the nearby blazar B2023+336. We investigate the hypothesis of source confusion between this blazar, known to have soft  $\gamma$ -ray emission, and the position of V404 Cygni.

### 3 Fermi-LAT OBSERVATIONS AND ANALYSIS

The goal of our analysis is to detect any  $\gamma$ -ray emission from V404 Cygni during both its 2015 outburst and August 2016, when Xing 20 claim detection of a  $\gamma$ -ray flare. We take 11.5 yr of *Fermi*-LAT data (inclusive of 2015–2016) with photons across the full effective energy range of the instrument: 100 MeV to 300 GeV.

We follow a standard data reduction chain using the FERMITOOLS (v1.2.23) and Pass 8 *Fermi*-LAT data, which has improved analysis methods and event reconstruction over previous versions. Following the method of Mattox et al. (1996), we execute a standard binned likelihood analysis using the parameters described in Table 1. Our binned analysis employs  $0.1^\circ$  spatial bins in RA and Dec (approximately the optimal resolution of the LAT at high energies), and we bin in energy with 8 bins per decade. Although unbinned analysis is typically used for time-series analysis of *Fermi*-LAT sources on short time-scales, we employ a binned analysis (as

recommended in the FermiTools Cicerone) because V404 Cygni is on the Galactic plane.

We then follow the method of Mattox et al. (1996) to use maximum likelihood estimation to fit a model to the data set on a bin-by-bin basis. We use the 4FGL catalogue and background parameters described in Table 1 to make a prediction for the number of photons per bin, and then iteratively push the parameters in the model closer to their likely values in order to improve our model’s accuracy.

We next free the normalization of all point sources within  $5^\circ$  of the central position of the ROI as well as the normalization of the Galactic and isotropic diffuse backgrounds. We then perform a full likelihood fit with respect to our freed sources and backgrounds.

We next employ some of the advanced analysis tools from FERMIPY (v0.19.0) (Wood et al. 2017), a PYTHON module that acts as a wrapper for the Science Tools, to further investigate the ROI. We first search for uncatalogued point sources using the FIND\_SOURCES algorithm, which fits a point source to each spatial bin in the model then calculates a likelihood TS for that point source. The TS is defined as the ratio of the likelihood of an alternative ( $\Theta_1$ ) and a null hypothesis ( $\Theta_2$ ); given by equation (1).

$$TS = 2 \ln \frac{L(\Theta_1)}{L(\Theta_2)}. \quad (1)$$

In this case, the null hypothesis is that there is no point source at a position, and the alternative hypothesis is that there is one. Through Wilks’ Theorem (Wilks 1938), the TS equates to a  $\chi^2$  statistic for  $k$  degrees of freedom.

Using this algorithm, we are able to search for new sources in an unbiased way. While we do not expect any long-term  $\gamma$ -ray emission from V404 Cygni, any point sources nearby that are uncatalogued will be added to the model, improving its accuracy. We set the TS threshold for the addition of a new point source to our model as 9 (a  $z$ -score of  $3\sigma$ ).

Given the proximity of B2023+336 to V404 Cygni in the sky, it is important to understand the characteristics of the blazar. Extended  $\gamma$ -ray emission is detected with *Fermi*-LAT in only two AGN: Fornax A Ackermann et al. (2016) and Centaurus A Abdo et al. (2010), both radio galaxies. We do not expect to see any extended emission from B2023+336, as it is a blazar, all of which are point sources. We use equation (1) to fit a radial Gaussian model as an alternative hypothesis against the null hypothesis of a point source model. The TS of extension for B2023+336 is calculated to be  $-0.01$ , strongly favouring the point source model over an extended one, as we would expect.

### 3.1 Spectral analysis

#### 3.1.1 Spectral analysis of B2023+336

B2023+336 is a notable  $\gamma$ -ray blazar, as it is one of the few that is seen through the Galactic plane, which is itself a luminous  $\gamma$ -ray emitter. As a result, although we expect some contamination of the photons from B2023+336 with those from the Galactic plane, which has a soft spectrum, use of the 8 yr Galactic background model should minimize this. In this section, we detail our spectral analysis of B2023+336, and compare it with the spectral analyses of the three  $\gamma$ -ray excesses. If the spectrum of any excess is significantly different from that of the blazar, we can consider this evidence that the excess is not a product of source confusion between B2023+336 and the position of V404 Cygni. If the spectra are similar this may imply source confusion, but this could be coincidental. Further evidence,



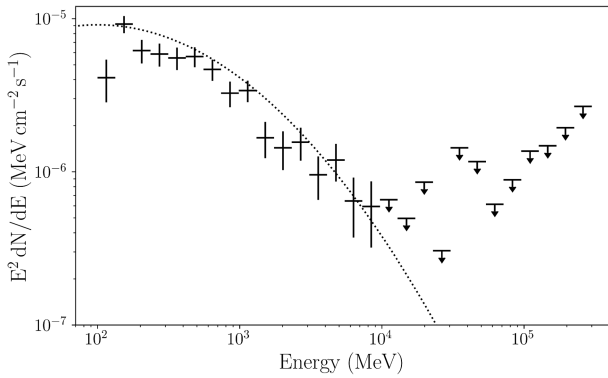


**Figure 1.** The spectral energy distribution of the blazar, B2023+336, with  $E^2 \frac{dN}{dE}$  flux shown plotted against bin energy. The dotted line shows our log-parabola fit, using the parameters described in Section 3.1.1, with a good fit to the data. This is unsurprising, as a log-parabola spectral shape is common among the LAT detected blazar population. We regard any bin which does not have a TS value of at least 4 as an upper limit.

such as correlated variability between B2023+336 and V404 Cygni, would be needed to draw a firm conclusion.

The spectral energy distribution of the blazar B2023+336 is given in Fig. 1, where 95 per cent confidence upper limits are fixed to bins with a  $z$ -score of less than 2. We find that the best fit to the bins is a log-parabola spectral shape, with a  $z$ -score of  $4.4\sigma$  against a power-law model. We also note that the power law with an exponential cutoff (PLEC) model fits to a  $4.0\sigma$  significance, so the difference in the goodness of fit between the log-parabola and PLEC is marginal. For the photon index of the spectral energy distribution (SED), we use the log-parabola index,  $\Gamma_{LP} = 2.74 \pm 0.08$ , which is in reasonable agreement with the photon index if a power law was fitted instead ( $\Gamma_{PL} = 2.65 \pm 0.05$ ). For the power law with exponential cutoff, we have a slightly lower photon index ( $\Gamma_{PLEC} = 2.20 \pm 0.05$ ) with an exponent index of  $0.66 \pm 0.19$ . Both the log-parabola and PLEC models provide similarly good fits over a power law, and all models describe the spectral shape in a similar way: flux generally anticorrelated with energy, commonly known as a soft  $\gamma$ -ray spectrum. There is a peak flux of  $9.22 \times 10^{-6} \text{ MeV cm}^{-2} \text{ s}^{-1}$  in the energy range 133 MeV to 177 MeV. We see a  $\gamma$ -ray flux cut-off at energies above 9.7 GeV. This spectral fit is compatible with that described in the 4FGL-DR2 (Abdollahi et al. 2020), where the log-parabola index is given as  $\Gamma_{LP} = 2.73 \pm 0.07$ . We also find no evidence for detectable variability of the spectral shape of B2023+336, leading us to believe that our best-fitting spectral parameters are an accurate description at all times.

### 3.1.2 Spectral analysis of the V404 Cygni $\gamma$ -ray excesses

The most significant of the three excesses reported in Loh 16 and Xing 20 is the August 2016 excess. The authors fit a power-law spectral model to this excess, although there are only four energy bins significant enough to be plotted. Their spectral fit has a power-law photon index of  $\Gamma_{PL} = 2.9 \pm 0.3$ , indicating soft  $\gamma$ -ray emission.

The other two excesses from June and August 2015, observed during the microquasar outburst of the binary system, also have published spectral analyses available. The June 2015 excess described by Loh 16 had a maximum flux of  $1.4 \pm 0.5 \times 10^{-6} \text{ photons cm}^{-2} \text{ s}^{-1}$ , and a soft power-law spectrum ( $\Gamma_{PL} = 3.5 \pm 0.8$ ). These spectral parameters were derived from the highest TS bin in their light curve. Piano 17 do not report the spectral parameters associated with their

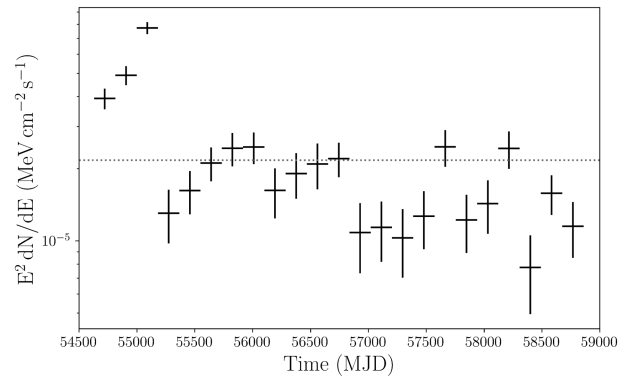


**Figure 2.** The light curve of the blazar B2023+336, with approximately 6 month time bins spread out across the observation period given in Table 1. The grey dotted line indicates a constant-flux model, which results in a poor fit to the observed data. This is expected given the blazar’s 4FGL catalogue variability index (V.I. = 116).

*Fermi*-LAT analysis, and assume a power-law spectrum of  $\Gamma_{PL} = 2.1$  for their AGILE analysis, which is the default for an AGILE source with low photon-statistics or an unknown spectrum (Pittori et al. 2009). Piano 17 show that the AGILE spectral parameters are consistent with the *Fermi*-LAT spectral parameters from Loh 16.

The August 2015 excess described by Xing 20 fig. 4 has an SED calculated in the same way as the August 2016 excess. A soft power law is fitted ( $\Gamma_{PL} = 2.5 \pm 0.4$ ), although like the August 2016 excess a limited number of bins is used (in this case 2).

### 3.1.3 Comparison of spectral analyses

All three  $\gamma$ -ray excesses have large uncertainties compared to that of the blazar that was observed over a much longer period. However, there is overlap between the uncertainties of the photon indices of the putative excesses and the blazar index, although statistics enable only a few energy bins to be used for the spectral fits of the excesses. The spectral similarity between the excesses and the blazar means that there is insufficient evidence to determine whether the origin of these excesses is B2023+336 or V404 Cygni. The similarity does suggest the possibility of source confusion, particularly in the case of the Xing 20 August 2015 and 2016 excesses where the photon indices lie closer to that of the blazar with smaller uncertainties than that determined during the June 2015 excess.

## 3.2 V404 Cygni variability analysis

As is generally true for FSRQs detected with *Fermi*-LAT (Meyer, Scargle & Blandford 2019), B2023+336 is variable, with a variability index of 116 (Ballet et al. 2020). A variability index greater than 72.44 indicates variability on the time-scale of months. This long-term variability is illustrated in Fig. 2, which shows a rise in flux from the start of the LAT data, with a peak flux of approximately  $8 \times 10^{-5} \text{ MeV cm}^{-2} \text{ s}^{-1}$  in early 2010, followed by a sharp drop-off with flux levels between 1 and  $3 \times 10^{-5} \text{ MeV cm}^{-2} \text{ s}^{-1}$  for succeeding bins. From 2015 June to December, the flux of B2023+336 plateaus at between 1 and  $2 \times 10^{-5} \text{ MeV cm}^{-2} \text{ s}^{-1}$  with all points within the 95 per cent confidence limit of one another, indicating a broadly steady  $\gamma$ -ray flux during the two apparent outbursts of V404 Cygni.

The three  $\gamma$ -ray excesses reported from V404 Cygni are reported on time-scales of less than 12 hr rather than months. In general

only the brightest sources seen with *Fermi*-LAT have variability that is detectable on short time-scales, one example being Cygnus X-3 (Abdo et al. 2009; Corbel et al. 2012). For V404 Cygni to be regarded as a  $\gamma$ -ray emitter, its emission must reach the  $5\sigma$  level which is conventional for a discovery over this time-scale. For reference, the blazar B2023+336 reaches a  $5\sigma$  significance over 12 hr in 2016 August, with a flux of approximately  $5 \times 10^{-4} \text{MeV cm}^{-2} \text{s}^{-1}$ . We would expect V404 Cygni to meet or exceed this flux threshold in order to reach  $5\sigma$ .

The June and August 2015 excesses reported by Loh 16 and Xing 20, respectively, do not reach the  $5\sigma$  level. Furthermore, the fact that the June 2015 excess was identified using a now outdated model and an older catalogue necessitates a repeat analysis of this period with the most recent models. Such an analysis, performed by Xing 20, failed to detect the 2015 events significantly, although as we have noted, differences in the analyses may explain this discrepancy.

Using the `Fermipy` light-curve algorithm, we execute a binned light-curve analysis of the *Fermi*-LAT data between 2015 June and 2015 September, a time period that covers the outburst of V404 Cygni. For our analysis, we have both background components freed in our model, along with the normalization of all sources within  $5^\circ$  of V404 Cygni's position (including B2023+336). We use a 12 hr independent binning scheme, and place a 95 per cent confidence upper limit on flux in any bin where the bin TS is less than 4 (corresponding to  $2\sigma$ , or  $p = 0.05$ ).

We have established that any potential excess may have a soft spectral energy distribution. The angular resolution of the *Fermi*-LAT is energy dependent, such that the PSF is worse at low energies. This is several degrees in the MeV range, where we expect both the flux of the blazar and also that of the binary to peak. As a measure to test for source confusion between the position of the binary and the blazar, we also execute an identical light curve, but at the position of the blazar  $0.3^\circ$  away. This will allow us to cross-correlate our results for the position of V404 Cygni with that of the blazar, to see if any excesses are also seen at the position of the blazar and to perform statistical tests of similarity between the light curve of the blazar and of V404 Cygni.

### 3.2.1 June 2015 excess

Fig. 3 shows a comparison between the V404 Cygni light curve (black) and B2023+336 (red)  $\gamma$ -ray flux and the TS value of each bin during the June 2015 outburst period, as well as the *Swift*-BAT light curve of V404 Cygni for this time. We do not see any  $\gamma$ -ray excess from the position of V404 Cygni during 2015 June, when Loh 16 report a  $4\sigma$  excess at the peak of the *Swift*-BAT light curve highlighted by the TS map in Fig. 4. This is not entirely surprising, as both Loh 16 and Piano 17 used older background models and an older catalogue for their analysis. A key difference between the 3FGL used by Loh 16 and the 4FGL used in our analysis (and Xing 20) is the addition of weighting in the maximum likelihood method employed in LAT analysis. The weighted maximum likelihood method better reflects the systematic uncertainties of the instrument, and results in larger parameter uncertainties and correspondingly smaller TS values. This could explain why an apparently significant time bin in the *Fermi*-LAT results of Loh 16 and Piano 17 is no longer seen when using the 4FGL, although this does not explain the AGILE result described in Piano 17. This result is in agreement with Xing 20, who similarly find no  $4\sigma$   $\gamma$ -ray excess in June, although there is a lack of information regarding the analysis parameters of Xing 20.

A further difference between our analysis and that of Loh 16 is that Loh 16 use an unbinned analysis. A binned analysis is preferred for sources on the Galactic plane; however, we also performed an unbinned analysis over the 12 hr period shown in Fig. 4, and find that this analysis agrees with the binned result.

### 3.2.2 August 2015 excess

Xing 20 report a separate  $4\sigma$   $\gamma$ -ray excess in August 2015 through use of independent binning. Two bins in our V404 Cygni light curve have significances above the upper limit threshold in 2015 August, ( $\sim$ MJD 57521), which is the same time period as that reported by Xing 20 in their analysis. While Xing 20 reports this excess at the  $4\sigma$  level, we find that one bin reaches the  $2\sigma$  level, and the second, consecutive, bin reaches  $3\sigma$ , with no corresponding rise in the count rate of the *Swift*-BAT light curve. We do not see a corresponding flux increase in the light curve of the blazar. Given that we use the same LAT catalogue and background models as Xing 20 it is likely that this discrepancy in results is down to the photon selection (we use energies greater than 100 MeV, and Xing 20 use energies greater than 300 MeV), and potentially other differences between our analysis and that of Xing 20.

With  $2\sigma$  and  $3\sigma$  consecutive bins over such a long time period we must consider the likelihood of an apparently significant result arising simply by chance. Out of 184 bins in our light curve of V404 Cygni, we find 2 bins with at least a  $2\sigma$  result. Looking at the  $3\sigma$  bin in particular, there is a 1 in 370 chance that this is a statistical anomaly. Considering that we have 184 separate bins, it is important to quantify the probability that this result arises by chance, as the number of bins is comparable to the chance probability.

The binomial distribution provides a suitable representation of our bins, and we calculate that the chances of finding exactly one  $3\sigma$  bin out of 184 to be 30.3 per cent, with a probability of finding at least one  $3\sigma$  result rising to 39.2 per cent. We therefore do not believe this August 2015 excess to be a significant  $\gamma$ -ray flare.

### 3.2.3 August 2016 excess

Xing 20 also claims a more significant  $7\sigma$   $\gamma$ -ray excess from V404 Cygni during 2016 August: a year after the outburst finishes. This is by far the most significant excess in their light curve. Fig. 5 shows the light curves of V404 Cygni and B2023+336 during 2016 August, around the result claimed by Xing 20. Using independent 12 hr binning, we do not find as high TS values as Xing 20 (although, as for the analysis of the August 2015 event, our photon selection and analysis parameters differ to those of Xing 20). Nevertheless, we do see three bins at the  $3\sigma$  to  $4\sigma$  level over a short period, with measurable fluxes. However, when we look at the light curve of B2023+336, we also detect fluxes in these bins and others around this time. As  $\gamma$ -ray fluxes are detected at both the binary and blazar simultaneously, this suggests confusion as to whether the flare originates from V404 Cygni or B2023+336.

There are no available multiwavelength observations of B2023+336 during the time of this detection. However, neither the optical AAVSO light curve or X-ray *Swift*-BAT light curve of V404 Cygni (Fig. 5) show any enhancement in their respective wavebands during 2016 August, nor is there any significant enhancement since the December 2015 flare. For V404 Cygni to form a jet which emitted  $\gamma$ -rays, we would expect an enhancement in the X-ray flux, similar to that seen in 2015 June (Fig. 3). As we do not see this, this suggests that there was no outburst from V404 Cygni at this time,

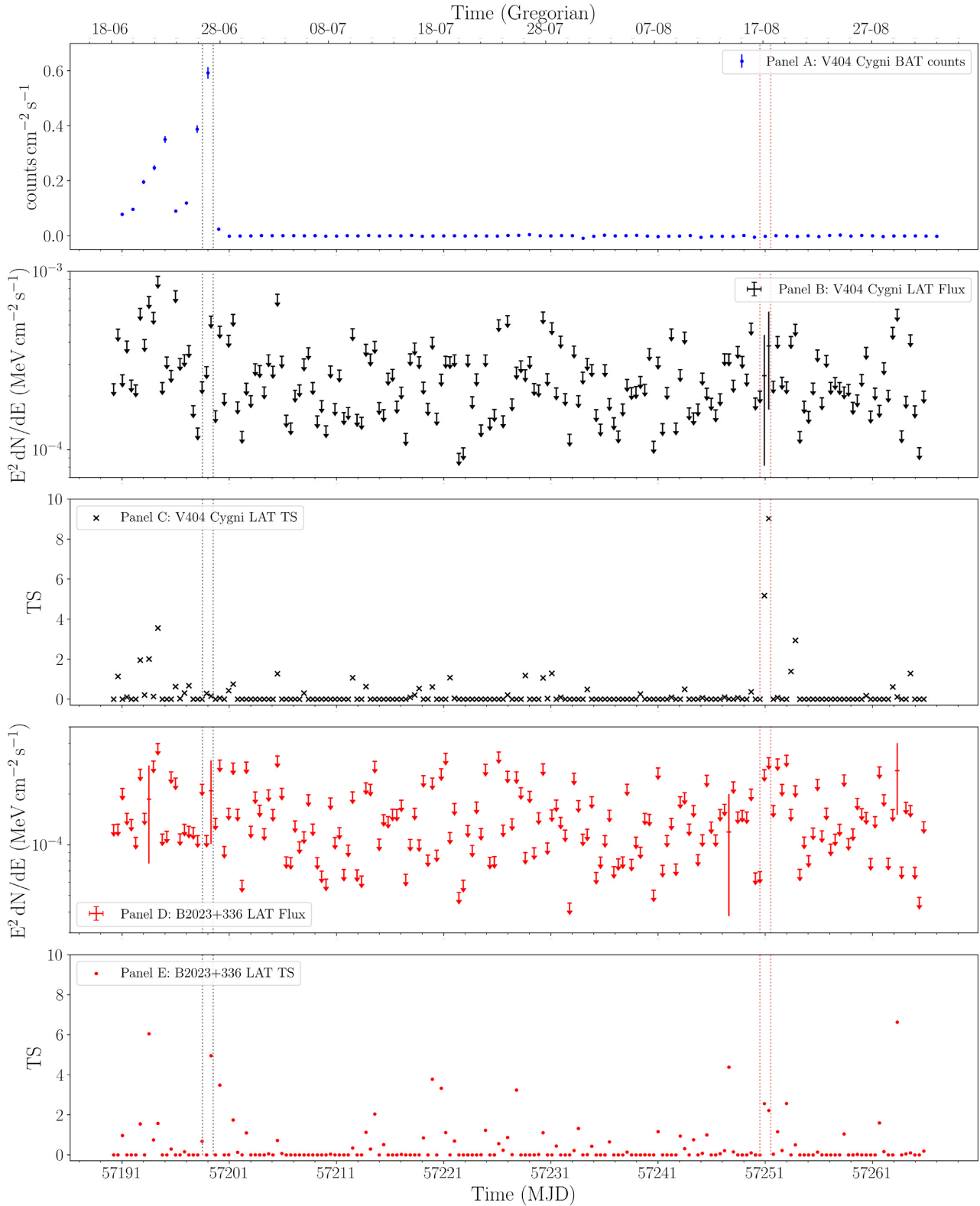


**Figure 3.** The light curves of V404 Cygni and B2023+336 during the 2015 outburst. Panel A shows the *Swift*-BAT light curve for V404 Cygni with daily binning. Panels B and C show the *Fermi*-LAT light-curve and TS values, respectively, for this period for V404 Cygni with 12 hr independent binning. Panels D and E show the *Fermi*-LAT light-curve and TS values, respectively, for B2023+336 with 12 hr independent binning. Units of time are Gregorian, and Modified Julian dates. The vertical grey dotted lines indicate the beginning and end period of the June 2015 excess, whereas the vertical pink dotted lines indicate the beginning and end period of the August 2015 excess.

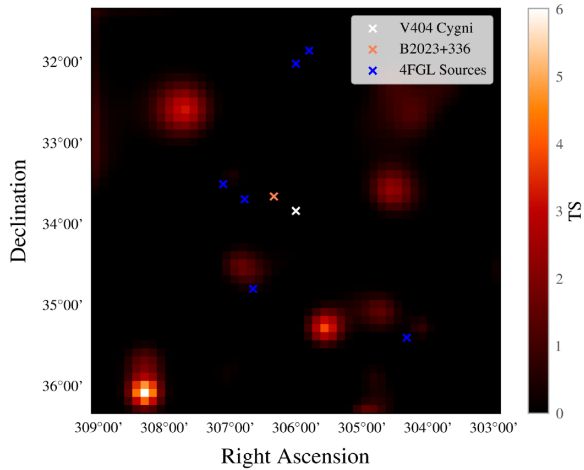


**Figure 4.** A TS map of the position of V404 Cygni over the 12 hr period (MJD 57199.25–57199.75) where Loh 16 describe their  $\gamma$ -ray excess (coincident with the peak in X-ray brightness). We observe no excess of  $\gamma$ -rays from the position of V404 Cygni during this time that cannot be accounted for by any of the neighbouring 4FGL sources, or the background models. This TS map is taken over the full effective *Fermi*-LAT energy range of 100 MeV to 300 GeV with  $0.1^\circ$  spatial bins.

supporting the hypothesis that the flare is from the blazar, not the binary.

### 3.2.4 Statistical tests of similarity

In order to look for similarity between the  $\gamma$ -ray emission of V404 Cygni and the blazar, B2023+336, we employ a 2-sample Kolmogorov–Smirnov (KS) test (Kolmogorov 1933; Smirnov 1948) in order to explore the hypothesis of source confusion. The 2-sample KS test essentially tests whether two numerical distributions are drawn from some common overall distribution, by calculating a KS statistic using equation (2).

$$D_{a,b} = \sup |F_{1,a(x)} - F_{2,b(x)}|. \quad (2)$$

Here,  $D_{a,b}$  is the KS statistic for two samples  $a(x)$  and  $b(x)$ , where the KS statistic is equal to the supremum of the absolute difference between the empirical distribution functions (EDFs) of the two samples. The EDFs for all of our samples are shown in Fig. 6. Alternative tests of similarity exist, such as the Mann–Whitney test (Mann & Whitney 1947), or the well-known Student’s t-test. However, we use the KS test as it is more powerful in detecting changes in the shape of the distribution, which is essential when analysing time-series data.

For the 2015 outburst period, we find  $D = 0.11$  indicating a  $p$ -value of  $p = 0.23$  for the hypothesis that the samples are drawn from separate distributions. This is unsurprising, as Fig. 6 shows that the EDFs for the blazar and binary at this time are not substantially different and although B2023+336 is a luminous  $\gamma$ -ray source, it is not known to be regularly detected on time-scales as short as 12 hr. Both sources are likely both dominated by the same noisy  $\gamma$ -ray background on the Galactic plane during the outburst, which provides the most likely source of the common distribution of TS values during the 2015 outburst.

For the 2016 outburst period, we find  $D = 0.425$  corresponding to  $p = 0.001$  for the same hypothesis, indicating a significant difference in the TS distributions of both the blazar and binary system. In Fig. 6, we see an increased probability of higher TS values for both systems

when compared to the 2015 outburst period where both systems are noise dominated, indicating increased  $\gamma$ -ray emission from both B2023+336 and the position of V404 Cygni. The plots of TS against time shown in Fig. 5 for August 2016 also show that the increased TS (and therefore flux) occurs for both systems at the same time, with the peak of both light curves occurring in the same bin indicating that this emission could have the same origin. Given that the EDF of B2023+336 shows an increased probability of higher TS values, and therefore more significant  $\gamma$ -ray emission than from V404 Cygni, this serves as statistical evidence at the  $3\sigma$  level that the origin of the August 2016 flare is B2023+336 rather than V404 Cygni.

In conjunction with the lack of X-ray emission observed by *Swift*-BAT from V404 Cygni during August 2016, we believe that there is sufficient evidence to state that the August 2016  $\gamma$ -ray flare originates from B2023+336 and not V404 Cygni. Any  $\gamma$ -ray emission observed from the position of V404 Cygni is a product of source confusion with B2023+336, due to the properties of the LAT itself (resolution, PSF, etc.), which are less precise at the lower energies where this flare occurs, as established in Section 3.1.2. Given that the LMXB system was in quiescence at this time, a blazar origin for this emission is much more likely.

### 3.2.5 Finding significant bins by chance

Xing 20 find the August 2015 and August 2016 excesses by running a light curve over 11.5 yr with 3-d independent binning, having also created but discarded light curves using 1-d and 6.5-d binning. This light curve is shown in Xing 20 fig. 3.

In addition to the  $\gamma$ -ray excesses described above, which we attribute to the large number of bins searched and source confusion with a B2023+336 flare, they find 10 other 3-d bins with TS values at the  $3\sigma$  level or above. The first four of these excesses (in time), labelled Period 1 in Xing 20 fig. 3, occur during the first 18 months of the *Fermi*-LAT mission. From our mission-long light curve of B2023+336, we can see that for the first 18 months of the *Fermi*-LAT mission, the flux is in an enhanced state with respect to all later bins. Both Loh 16 and the *Fermi* All-Sky Variability Analysis team (Ackermann et al. 2013) also report on the enhanced state of the blazar. As Period 1 overlaps with the enhanced flux state of the blazar, and considering our evidence with regards to source confusion, particularly during flares, we believe the  $\gamma$ -ray flux enhancement during Period 1 to be from the blazar.

Having accounted for the flux excesses in Period 1 and the August 2015 and 2016 excesses, we note that six other  $\gamma$ -ray excesses are described in Xing 20 fig. 3. As this light curve covers 11.5 yr, with 3 d binning, we estimate there to be approximately 1400 bins in this time. We are able to employ the binomial distribution to predict how many  $\gamma$ -ray excesses we are likely to occur at the  $3\sigma$  level. We find that there is an 9.25 per cent chance of finding these six  $\gamma$ -ray excesses by chance, indicating a strong possibility that there is no  $\gamma$ -ray emission from V404 Cygni shown in the Xing 20 fig. 3 light curve that cannot be accounted for with either source confusion with B2023+336 or by considering the effect of apparently significant bins arising by chance.

## 4 DISCUSSION

Using recent *Fermi*-LAT background models and IRFs, together with the 4FGL, we analyse the position of V404 Cygni in the Pass 8 *Fermi*-LAT data. Previous works Loh 16, Piano 17, and Xing 20 have identified three  $\gamma$ -ray excesses over the course of the *Fermi*-LAT



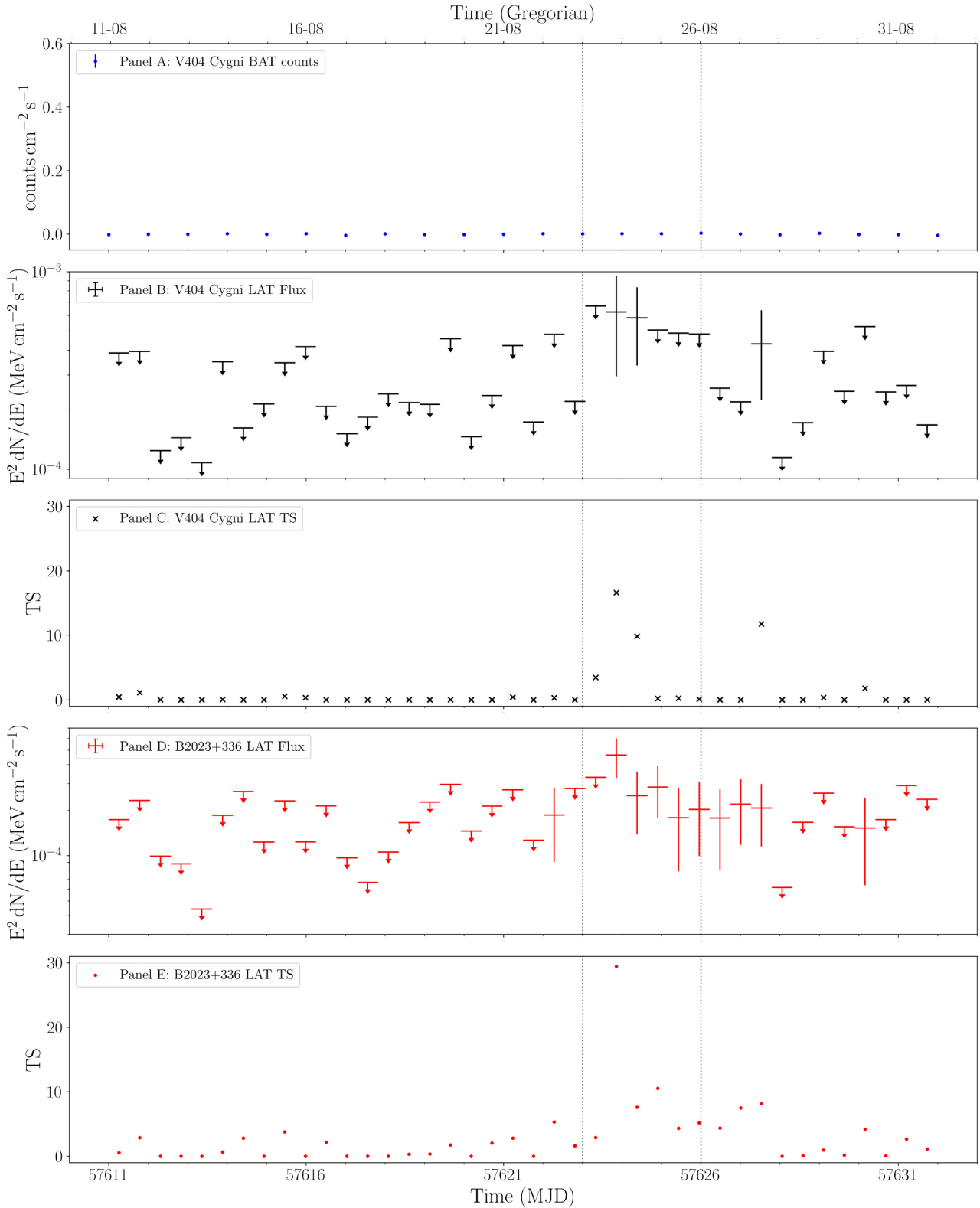


**Figure 5.** The light curves of V404 Cygni and B2023+336 during 2016 August, when [Xing 20](#) claim their detection of V404 Cygni. Panel A shows the *Swift*-BAT light curve for V404 Cygni with daily independent binning. Panels B and C show the *Fermi*-LAT light-curve and TS values, respectively, for this period for V404 Cygni with 12 hr independent binning. Panels D and E show the *Fermi*-LAT light-curve and TS values, respectively, for B2023+336 with 12 hr independent binning. Units of time are Gregorian, and Modified Julian Dates. The vertical grey dotted lines indicate the beginning and end of the 3-d time bin [Xing 20](#) used to identify the August 2016 excess. We also observe  $\gamma$ -ray emission outside this time period at comparable TS values.



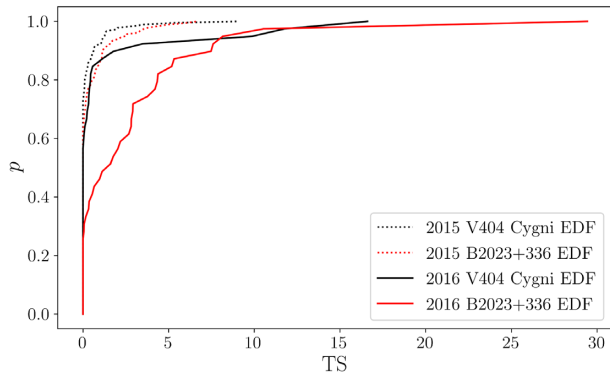


**Figure 6.** The EDFs of V404 Cygni and B2023+336 during the 2015 outburst and the 2016 flare for the TS of each time bin. The B2023+336 and V404 Cygni distributions in 2015 are very similar, and are dominated by the noisy background. During 2016, the V404 Cygni distribution reaches a higher peak TS, with a higher probability of increased TS values over 2015. The most significant emission comes from B2023+336 during 2016, where we see a TS peak higher than the V404 Cygni distribution.

mission which could be indicative of high energy  $\gamma$ -ray emission from V404 Cygni.

The first of these excesses is described by Loh 16 and Piano 17, and occurred in June 2015 coincident with the hard X-ray peak of the outburst, during the peak of the AAVSO optical light curve, and shortly following the peak radio emission. The background models, catalogue, and IRFs used in this analysis are now superseded by more accurate models, and when we carry out our own binned (and unbinned) analyses, we find no significant  $\gamma$ -ray emission. We believe this  $\gamma$ -ray excess to be a product of the older models available at the time for *Fermi*-LAT data analysis, rather than a statistically significant detection. This is supported by the fact that the peak significance only reaches  $4\sigma$  in the Loh 16 analysis, and not the conventional  $5\sigma$  level required to claim a detection, although a slightly lower significance may be acceptable in light of multiwavelength data supported by theory. While there appears to be no significant excess from V404 Cygni as seen with *Fermi*-LAT based on our analyses, this does not discount the excess observed within the AGILE data discussed in Piano 17, which remains the strongest independent evidence for  $\gamma$ -ray production in V404 Cygni.

The next of these excesses is a separate  $4\sigma$  excess at the end of the outburst in August 2015, claimed by Xing 20. Unlike the first, there is no corresponding X-ray enhancement, but we do also see this excess in our own analysis. However, a wider issue with apparently significant bins arising by chance both in our own light curve (Fig. 3) and the work of Xing 20 leads us to believe that this is probably a chance occurrence.

The final, and most significant, claim of  $\gamma$ -ray emission occurring from V404 Cygni was the  $7\sigma$  August 2016 excess reported by Xing 20, after the X-ray outburst had finished. We find that this is more than likely a product of source confusion with B2023+336, which also appeared to be active at this time. Given that the  $\gamma$ -ray emission from B2023+336 is present longer, more consistently, and more significantly than that reported from the position of V404 Cygni, and the spectral similarity between this excess and the spectrum of B2023+336, we believe that this  $\gamma$ -ray excess is a product of source confusion between the blazar and V404 Cygni. This is supported by the fact that V404 Cygni was in quiescence at this time, and is not likely to become

an active microquasar again for approximately another decade or two.

A definitive identification of  $\gamma$ -ray emission from a new binary system would be an important result, as so few are detected with *Fermi*-LAT. An interesting prospect in this respect is AMEGO (McEnery et al. 2019), proposed to launch in 2030. As AMEGO will operate in the MeV range, where we would expect V404 Cygni to emit  $\gamma$ -rays, and will operate with greater sensitivity and resolution than *Fermi*-LAT. It is very possible that, if V404 Cygni becomes active again, AMEGO will make a significant detection. The 2030 target launch date, and the 1 to 2 decade microquasar cycle of V404 Cygni, means the next time this system becomes active the scientific community will hopefully have a clearer picture as to the high energy physics involved in such a system.

## ACKNOWLEDGEMENTS

The authors would like to acknowledge the excellent data and analysis tools provided by the NASA *Fermi* collaboration, without which this work could not be done. In addition, this work has made use of the SIMBAD data base, operated at CDS, Strasbourg, France, and Montage, funded by the National Science Foundation. We would also like to thank Chris Done, Matthew Capewell, and Jamie Holder for useful discussions. We thank the referee for constructive feedback in producing this work.

MH acknowledges funding from Science and Technology Facilities Council (STFC) PhD Studentship ST/S505365/1, and PMC and CBR acknowledge funding from STFC consolidated grant ST/P000541/1.

## DATA AVAILABILITY

All data used within this paper are from the NASA *Swift* and *Fermi* missions. It is publicly available for download from the relevant servers on the NASA website. The *Fermi*-LAT data analysis tools are also publicly available from the same site.

## REFERENCES

- Abdo A. A. et al., 2009, *Science*, 326, 1512  
 Abdo A. et al., 2010, *Science*, 328, 725  
 Abdollahi S. et al., 2020, *ApJS*, 247, 33  
 Ackermann M. et al., 2013, *ApJ*, 771, 57  
 Ackermann M. et al., 2016, *ApJ*, 826, 1  
 Ahnen M. L. et al., 2017, *MNRAS*, 471, 1688  
 Araudo A. T., Bosch-Ramon V., Romero G. E., 2009, *A&A*, 503, 673  
 Archer A. et al., 2016, *ApJ*, 831, 113  
 Atwood W. B. et al., 2009, *ApJ*, 697, 1071  
 Ballet J., Burnett T. H., Digel S. W., Lott B., 2020, preprint (arXiv:2005.11208[astro-ph])  
 Barthelmy S. D., D’Ai A., D’Avanzo P., Krimm H. A., Lien A. Y., Marshall F. E., Maselli A., Siegel M. H., 2015, GCN Circ., 17929, 1  
 Bodaghee A., Tomsick J. A., Pottschmidt K., Rodriguez J., Wilms J., Pooley G. G., 2013, *ApJ*, 775, 98  
 Bosch-Ramon V., Romero G. E., Paredes J. M., 2006, *A&A*, 447, 263  
 Corbel S. et al., 2012, *MNRAS*, 421, 2947  
 Dubus G., 2006, *A&A*, 456, 801  
 Duerbeck H. W., 1988, Bull. Inf. Cent. Donnees Stellaires, 34, 127  
 Fabrika S., 2004, Astrophys. Space Phys. Rev., 12, 1  
 Fender R. P., Belloni T. M., Gallo E., 2004, *MNRAS*, 355, 1105  
 Han X., Hjellming R. M., 1992, *ApJ*, 400, 304  
 Kara E. et al., 2012, *ApJ*, 746, 159  
 Khargharia J., Froning C. S., Robinson E. L., 2010, *ApJ*, 716, 1105

- Kitamoto S., Tsunemi H., Miyamoto S., Yamashita K., Mizobuchi S., 1989, *Nature*, 342, 518
- Kolmogorov A. N., 1933, *G. Ist. Italiano degli Attuari.*, 4, 83
- Leser E. et al., 2017, *Proceedings of 35th International Cosmic Ray Conference*, 35, 717
- Loh A. et al., 2016, *MNRAS*, 462, L111 (Loh 16)
- McEnery J. et al., 2019, *BAAS*, 51, 245
- Makino F., 1989, *Int. Astron. Union Circ.*, 4782, 1
- Mann H. B., Whitney D. R., 1947, *Ann. Math. Stat.*, 18, 50
- Mattox J. R. et al., 1996, *ApJ*, 461, 396
- Meyer M., Scargle J. D., Blandford R. D., 2019, *ApJ*, 877, 39
- Motta S. E. et al., 2017, *MNRAS*, 471, 1797
- Oates S. R. et al., 2019, *MNRAS*, 488, 4843
- Orellana M., Bordas P., Bosch-Ramon V., Romero G. E., Paredes J. M., 2007, *A&A*, 476, 9
- Piano G., Munar-Adrover P., Verrecchia F., Tavani M., Trushkin S. A., 2017, *ApJ*, 839, 84 (Piano 17)
- Pittori C. et al., 2009, *A&A*, 506, 1563
- Richter G. A., 1989, *Inf. Bull. Var. Stars*, 3362, 1
- Rodriguez J. et al., 2015, *A&A*, 581, L9
- Roques J.-P., Jourdain E., Bazzano A., Flocchi M., Natalucci L., Ubertini P., 2015, *ApJ*, 813, L22
- Smirnov N., 1948, *Ann. Math. Stat.*, 19, 279
- Tavani M. et al., 2009, *Nature*, 462, 620
- Tomsick J. A. et al., 2008, *A Population Explosion: The Nature & Evolution of X-ray Binaries in Diverse Environments, Vol.1010*, p. 13
- Wagner R. M., Starrfield S. G., Cassatella A., Hurst G. M., Mobberley M., Marsden B. G., 1989, *Int. Astron. Union Circ.*, 4783, 1
- Wagner R. M., Kreidl T. J., Howell S. B., Starrfield S. G., 1992, *ApJ*, 401, L97
- Wilks S. S., 1938, *Ann. Math. Stat.*, 9, 60
- Wood M., Caputo R., Charles E., Di Mauro M., Magill J., Perkins J., 2017, *Proceedings of 35th International Cosmic Ray Conference*, 35, 824
- Xing Y., Wang Z., 2020, preprint ([arXiv:2006.15790](https://arxiv.org/abs/2006.15790))
- Zanin R., Fernández-Barral A., de Oa Wilhelmi E., Aharonian F., Blanch O., Bosch-Ramon V., Galindo D., 2016, *A&A*, 596, A55
- Zdziarski A. A., Malyshev D., Chernyakova M., Pooley G. G., 2017, *MNRAS*, 471, 3657

This paper has been typeset from a  $\text{\TeX}/\text{\LaTeX}$  file prepared by the author.